

Assessing Bearing Health for Helicopter Power Train Systems

Harrison H. Chin

Eric Mayhew and David L. Green

Applied Concept Research, Inc.
Bedford, MA 01730

Goodrich Corporation
Fuel & Utility Systems
Vergennes, VT 05491

Abstract

Bearings are critical components in helicopter power train systems. A failing bearing not only could jeopardize the safety of flight but also induce collateral damages, adding additional maintenance costs. Detecting bearing faults remains a challenge because of feeble signatures generated by bearings that are often masked by other noise in the power train system. HUMS data collected to date from 30 U.S. Army BlackHawk helicopters enables us to learn more about bearing fault behaviors in an operational environment. The lessons learned in this program will allow us to further advance bearing health assessment methodology and to achieve Condition-Based Maintenance.

Introduction

The U.S. Army is in the process of transitioning from current Time-Based Maintenance (TBM) to Condition-Based Maintenance (CBM) for their UH-60L and other helicopters. Unlike TBM where maintenance or retirement of components is performed based on a fixed operating hour schedule, CBM requires timely replacement or repair of components before they fail (i.e., unscheduled maintenance). It can be argued that CBM of a helicopter power train system requires automated diagnostics and prognostics to provide current component status, and predict the time remaining before the useful life is consumed. This new maintenance philosophy promises to reduce the overall maintenance costs while improving aircraft readiness.

Bearings are one of the power train components that will be subject to CBM. Early detection of bearing degradations allows the maintainer to plan corrective actions so as to minimize the impact to readiness, and in many cases minimize collateral damages. Planning lead time allows the replacement assembly to be ordered and delivered before the aircraft becomes unserviceable, and allows the replacement effort to be accomplished when the technicians, space, and special tools are available. Similarly, minimizing collateral damages has the potential of minimizing the cost and foreshortening the time required to overhaul the parent assembly.

The Army has been taking several concrete steps toward CBM, including a battalion-level demonstration of the Goodrich Integrated Mechanical Diagnostics Health and Usage Monitoring System (IMD HUMS) installed on 30 UH-60L BlackHawk helicopters [1]. The Goodrich IMD HUMS provides a mix of industry standard and privately developed diagnostics and management techniques. Much of the privately developed technology is centered in the areas of rotor track and balance (RTB) and automated mechanical diagnostics (AMD). This technology has been developed through years of research and development in concert with government personnel in test stand environments and on aircraft data collection.

Techniques and concepts have been developed for measuring mechanical state and assessing mechanical health. These techniques have been incorporated into the IMD HUMS and are now gaining large scale application. Exposing the general rules, developed on a small sample set and test cells, to a large sample size has uncovered areas that need additional interpretation. Refining the algorithms and techniques has always been an expected stage of the pre-planned deployment for this technology.

Automated Mechanical Diagnostics (AMD) is a unique challenge for several reasons. In contrast to main rotor out of balance conditions, mechanical faults are rare in normal operation. It is a challenge to provide evidence, of a reliable diagnostic system, in the absence of mechanical faults. Without operational evidence, theory and more importantly test cell data is all that can be provided. Navy and Goodrich efforts have led to a compilation library of various fault signatures. The efforts in understanding theoretical responses to simple

mechanical anomalies and measuring the response on a controlled test facility have driven the implementation as seen today on the IMD HUMS AMD function. The second major challenge is to properly model the relationship of measured responses to component state based on visual representations of the data.

The planned approach Goodrich has taken to mitigate the effects of development on a finite sample size is to incrementally update thresholds and data blending techniques as the fleet data is acquired. In the absence of faulted data, deviation from fleet normal is being reported. Provided that enough evidence has been gathered to confidently say that the measurements are sensitive to degradation modes, deviation from statistical fleet normal is interpreted as approaching or achieving fault detections.

In addition to HUMS ground station software provided to the Army personnel, Goodrich has developed a versatile engineering software utility called Mechanical Diagnostics Analysis Toolkit (MDAT) that enables detail analysis of HUMS data. Since 2002, the MDAT has been used to conduct detailed data analysis and accomplish rapid prototyping needed to respond to the unique challenges associated with operations of the UH-60L power train in a variety of operational environments. This data has given the researchers the means to refine and optimize HUMS functionalities, including bearing diagnostic algorithms. Furthermore, the data also serves as the basis for multi-aircraft statistical analysis, as well as for the development of advanced prognostic algorithms.

Given the number of aircraft involved and the amount of data generated, a health evaluation tool has been developed to perform health assessment for every power train component automatically. With the aid of this tool, aircraft with the worst component(s) can be readily identified for special analysis, the results of which have been used to validate automated detections.

In this paper, issues related to bearing health assessment are discussed, which reveal the similarities and dissimilarities between theoretical understandings and actual observations of bearing degradation. Several important findings related to IMD HUMS bearing data are described.

The Bearing Challenge

Detecting bearing faults remains a challenge. A faulted bearing generates minute vibrations that are often masked by other noise sources in the power train. The bearing signatures are also subject to a certain amount of scatter due to variability in installation and operating

environment. This further complicates the efforts to properly detect and quantify bearing faults.

Many bearing monitoring techniques such as vibration analysis, acoustic emission, and oil debris analysis have been developed over the past decades to address this problem. Among them, vibration monitoring has been proven to be a reliable and cost-effective technique for on-board implementation. Onboard implementation allows data to be downloaded upon landing and in some cases allows onboard alerts of impending in-flight failures. This last feature requires a detection system that is comprehensive, extremely accurate and highly reliable.

Bearing Fault Progression

Bearing fault progression typically can be described by 4 distinct stages [2]. Symptoms often start at high frequency excitation and move to lower frequencies as damage progresses, as shown in Figure 1.

In Stage I, there are some ultra high frequency activities in the ultrasonic region (Zone 4), which represent the “spike energy” produced by bearing micro-defects. It requires a sensor specifically designed to detect such spikes in this region. Visual inspection of the bearing at this stage may not show any identifiable defects.

In Stage II, the faulty bearing begins to generate signals associated with natural frequencies of the bearing parts as they are being excited by the defects. It produces a notable increase of signals in Zones 3 and 4 in this stage. Beginning signs of defects will be found upon inspection.

Fundamental bearing defect frequencies start to appear in Stage III of bearing damage. There may be higher harmonics of these frequencies, depending upon the quantity of defects and their distribution around the bearing races. These frequencies are sometimes modulated by the shaft frequency as the defects interact with the shaft rotation. Bearing defect frequencies and their harmonics are observed in Zone 2. Signals in Zones 3 and 4 continue to grow throughout this stage.

Stage IV is the last condition before catastrophic failure of the bearing. This stage is associated with numerous modulated fundamental frequencies and harmonics, indicating the defects are distributed around the bearing races. Due to the increased degradation of the bearing the internal clearances become larger, which then allow the shaft to vibrate more freely. Consequently an increase in shaft fundamental frequency and harmonics is observed, which can be associated with imbalance, misalignment, and/or looseness of the shaft. Toward the

end of Stage IV, the bearing fundamental frequencies will actually decrease and be replaced with an elevated noise floor or “hay stack” at higher frequencies. Signals in Zone 4 will decrease followed by a significant increase just prior to catastrophic failure [2].

Bearing Vibration Monitoring

Generally speaking vibration monitoring is the most widely used technique for detecting rolling element bearing failures. Vibration characteristics from bearing faults are well documented, and proven techniques to extract such information are available [3][4]. Furthermore the accelerometers used for bearing monitoring are also suitable for monitoring shafts and gears in the power train system. This makes it the most cost-effective solution without additional hardware.

In a rolling element bearing, the fundamental shaft vibration is supplemented by the mechanics inherent with the additional moving bearing parts. A healthy bearing generates very little or no vibration while a damaged bearing has a distinct vibration signature. This vibration signature is typically proportional to the bearing load.

Bearing fault development typically starts with a crack or spall in the outer race. These faults can usually be detected from several months up to half a year before they become critical. These faults may become smoother after a while. Inner race faults are often developing as a result of an outer race fault, and may be detected some weeks before they become critical. Inner race faults often shows side bands due to modulation. Faults on rolling elements and cages are a sign of the final fault development of a bearing. Bearings with these faults will often last for only a few hours [5].

The bearing faults can be detected with envelope analysis technique which reveals the periodic impulses produced by a bearing defect. Envelope analysis demodulates the vibration signal in a narrow frequency bandwidth (in Zone 2), typically centered on a structural resonance. The time period between these periodic impulses, which are enhanced by the resonance, gives an indication of the location and nature of the bearing damage because the impulse frequencies can be traced back to the four bearing defect passage frequencies: cage, ball/roller, outer race, and inner race.

The above four bearing defect frequencies can be calculated based on the measured shaft speed and bearing geometric parameters: pitch and rolling element diameters, number of rolling elements, and contact angle. Figure 2 shows the geometric parameters for a ball bearings and equations for the defect frequencies

[5]. Bearing manufacturers normally supply the geometric data and/or the bearing defect frequency ratios as part of the bearing specifications. The actual frequencies may differ slightly due to loads and slippage but are expected to be close to the calculated frequencies. However the calculated frequencies become unreliable if the ratio between the radial and axial forces is not constant (e.g., change in contact angle) or there is excessive ball sliding (e.g., loose clearance fit).

In addition to vibration monitoring, the following techniques are often used for bearing diagnostics:

- Acoustic or ultrasound emission sensors designed to detect bearing micro-defect signatures in the ultra high frequency range (above 250 kHz).
- Thermal probes to detect any temperature changes for a bearing. Increase in measured temperatures normally indicates a possible loss of lube or excessive bearing defects that lead to increased friction between rolling elements, which can then result in bearing failures.
- Oil debris monitor and chip detector are used to detect the presence of wear metals and to infer the integrity of lubricant. Oil analysis using atomic emission or atomic absorption instruments is designed to detect the presence of wear metals in extremely low concentrations by spectrometric analysis of fluid samples.

The IMD HUMS utilizes the envelope analysis technique on vibration data acquired from multiple high frequency accelerometers to determine bearing health. Several Condition Indicators (CIs) are extracted from the envelope data and subsequently fused into a Health Indicator (HI) to reflect the health of each bearing. The HI has a value between 0 (healthy) to 1 (failure).

Bearing Health Analysis

One of the primary goals of the Army HUMS demonstration program is to verify and validate the IMD HUMS CIs and HIs with regard to their diagnostics performance. Contrary to test-stand environment [6], performing component health management in an operational environment for 30 aircraft is a complex task, due to different stages of component usage and aircraft-to-aircraft variability. Each aircraft’s power train system contains more than 70 bearings that need to be monitored. That represents a total of over 2,100 individual bearings for 30 aircraft.

To automate the health assessment process, a comparative analysis tool has been developed. The

result of this analysis is a list of components that show elevated and/or significantly increasing HIs. The HIs in the list are the result of blending a set of selected bearing CIs by employing both rule-based and data-driven statistical approaches. The list then serves as the basis for further engineering investigations on those components.

With the aid of this comparative analysis, several bearings have been identified as having potential faults. One such bearing is the Intermediate Gear Box (IGB) Input Thrust Bearing on one of the aircraft. The health of this bearing from the 30 aircraft is shown in Figure 3, ranked according to their HIs. It can be seen that among the 30 aircraft, the HI of AC # 11 has the highest value (nearly 0.9) that is more than 4 times higher than the second highest aircraft.

This elevated HI prompted a more comprehensive engineering analysis on the subject bearing. The CIs and, in some acquisitions, raw/intermediate data can be viewed and extracted from the MDAT tool. Figure 4 shows a screen shot of the MDAT tool displaying the CIs for the subject bearing, where an increasing trend can be observed on several CIs.

To confirm a bearing fault, the CIs must be traced back to one or more of the bearing defect frequencies mentioned earlier. For this, envelope spectrums from several acquisitions were extracted and examined. Figure 5 shows the topographical plot of 147 envelope spectrum waterfall, sorted by the averaged engine torque. Several distinct tones associated with bearing frequencies are seen throughout the plot, including the cage, outer race (OR), inner race (IR), and 2X OR. In addition to the bearing frequencies there is also the gear mesh (GM) frequency which appears more consistently at higher torque.

Figure 6 shows the comparison between one of AC # 11 envelope spectrums and one from AC # 6, representing a healthy bearing. The OR and 2X OR tones can be clearly identified in the AC # 11 spectrum, accompanied by a higher noise floor.

The above analysis has demonstrated the IMD HUMS bearing diagnostics capability in identifying a faulted bearing. The next step is to minimize the scatter in CIs so a more consistent HI can be obtained as oppose to the one shown in Figure 7.

Upon close inspection of the calculated OR frequencies vs. the actual frequencies in the envelope spectrums, it was found that the actual frequency is on average 1.5 Hz lower than the calculated (see Figure 8). This suggests that the bearing geometric parameters used to

calculate the bearing frequencies are not exact, or may be due to excessive slippage in the bearing. The only possible parameter to change is the contact angle that also affects the other three bearing frequencies. The only other visible frequency in the spectrum is the IR frequency which showed the actual frequency is on average 1.87 Hz higher than the calculated. By reducing the contact angle by a few degrees in the equations, a much better fit was achieved for both OR and IR frequencies. Such fine-tuning of the bearing defect frequencies will enable us to obtain more consistent CIs and HIs.

Another bearing example involves the shifting of a bearing defect frequency. It is generally assumed that the four bearing defect frequencies are approximately constant for a given shaft speed. This is because each of those frequencies is expressed as a function of shaft speed and bearing geometric parameters only, as shown in the equations in Figure 2.

Recent observations on one aircraft (AC # 7) reveal several elevated ball energy CI values of Right Input Spiral Bevel Pinion Gear Ball Bearing (see Figure 9). These high data points far exceed the nominal data scatter observed on other aircraft. An in-depth analysis was conducted to determine the source of these high data points.

After examining the envelope spectrums associated with this bearing, the ball frequency and its shaft modulation frequencies were found to vary with torque, that is, higher torques produce higher frequencies, as shown in Figure 10. It also shows that there is very little vibration when the engine torque falls below 40%.

Figure 11 shows the ball frequency as a function of the right engine torque. The ball frequency changes from low to high with increasing torque, with a value between 1,720 Hz (40% Q) and 1,920 Hz (80% Q). The expected frequency is around 1,820 Hz, which corresponds to roughly 50% Q.

It is postulated that there is a change of ratio between the axial and the radial load when different power is applied to the bearing from the shaft. In addition, since the defect has compromised the internal clearance (i.e., larger gap has developed) and therefore it promotes more excessive ball sliding that can also affect the defect passage frequency.

In addition to the two cases described above, this comparative analysis has also uncovered several instances where tail drive shaft bearing HIs are elevated but no actual bearing defect tone was found. Instead, the HIs are driven by high level of broad band noise.

They later were identified by field engineers as improper shimming that produced excessive end-load on the bearing. Other installation problems can also produce high shaft vibration which in turn produces looseness and higher load on the bearing. The above installation problems are believed to have contributed to accelerate bearing wear and premature failures. The ability of IMD HUMS to identify installation problems is key to prolonging bearing life.

Conclusions

The decision to build the Army IMD HUMS program around 30 aircraft that have accumulated an average of 2,000 flight hours, and were involved in a variety of typical tactical operations has been validated by the results accumulated to date. The ability to make on-aircraft detections of bearing degradation is a current capability of the IMD HUMS as installed on the UH-60L aircraft.

Several analysis tools/techniques such as MDAT and comparative analysis have been shown to be effective in HUMS data analysis and interpretation. MDAT has been proven to be a valuable tool in the control of data scatter, and provides an integrated development environment for rapid prototyping trending techniques that are essential to advanced fleet wide diagnostics.

Several important findings related to bearing faults have been identified by the above program, which were not observed during earlier controlled test cells or single aircraft testing. These findings give us an insight into bearing fault behaviors in a complex helicopter power train system under real-life operations. They also allow us to refine/develop more efficient and reliable diagnostic/prognostic models, which is a crucial step in the transition to CBM.

Significant findings of IMD HUMS bearing data and their implications are summarized below:

- The onboard detection of the faulted IGB input thrust bearing and post-flight analytical validation confirms the ability of the IMD HUMS to automatically detect progressive bearing faults.
- The tail rotor drive shaft bearing detection reported above validates the IMD HUMS ability to automatically detect improperly installed drive train bearings.
- The improvement of bearing algorithms to assure reliability of fault degradation detection in the presence of broad band noise demonstrates the ability of the AMD bearing

algorithms to function correctly in a high noise environment.

- Airworthiness is assured by the AMD because of early detection so as to avoid flight with a bearing in a near failure status, as well as automatic in-flight detection and reporting of extremely high HIs that indicate the probability of an imminent bearing failure.
- Battalion level CBM is facilitated by the ability to trend HIs so as to predict the service life remaining.
- Fleet management CB logistics is facilitated by early detection, tracking, and reporting the status of bearings showing progressive degradation.

References

- [1] Dora, Ray, Wright, J., Hess, R., and Boydston, B., "Utility of the IMD HUMS in an Operational Setting on the UH-60L Blackhawk," *AHS International Forum 60*, Baltimore, MD, 2004.
- [2] "Rolling Element Bearings," *STI Field Application Note*, Sales Technology, Inc., League City TX.
- [3] Randall, R. R., Antoni, J., and Bonnardot, F., "Recent Advances in Bearing Diagnostic Techniques for Helicopter Gearboxes," *Proceedings of the 58th Mechanical Failures Prevention Technology Meeting*, Virginia Beach, VA, 2004.
- [4] Chin, H., "Automated Bearing Fault Detection with Unsupervised Neural Nets," *Proceedings of the 49th Mechanical Failures Prevention Technology Meeting*, Virginia Beach, VA, 1995.
- [5] Eisenmann, R. C and Eisemann R. C., Jr., *Machinery Malfunction Diagnosis and Correction*, ISBN 0-13-240946-1, Prentice Hall PTR, Upper Saddle River, NJ 07458, 1998.
- [6] Hess, A., Hardman, W., Chin, H., and Gill, J., "The US Navy's Helicopter Integrated Diagnostics System (HIDS) Program: Power Drive Train Crack Detection Diagnostics and Prognostics, Life Usage Monitoring, and Damage Tolerance; Techniques, Methodologies, and Experiences," *NATO Conference*, 1999.

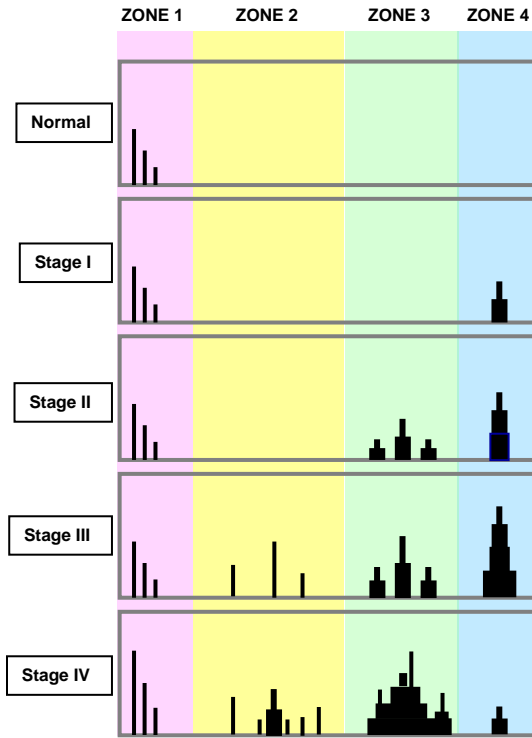


Figure 1. Typical bearing failure progression which can be described by 4 stages with signatures in 4 zones.

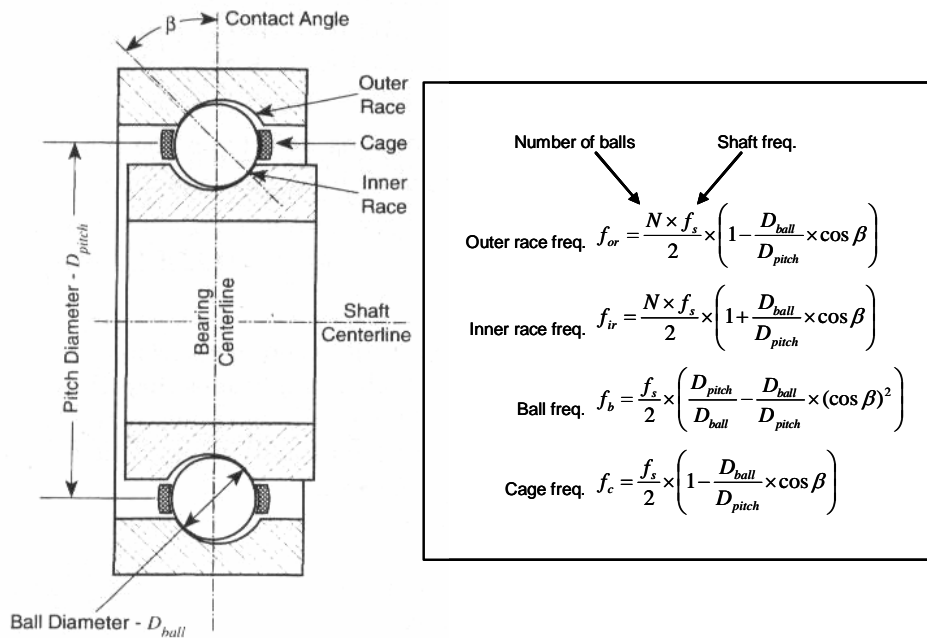


Figure 2. Rolling element bearing geometry and defect frequencies (courtesy of [5]).

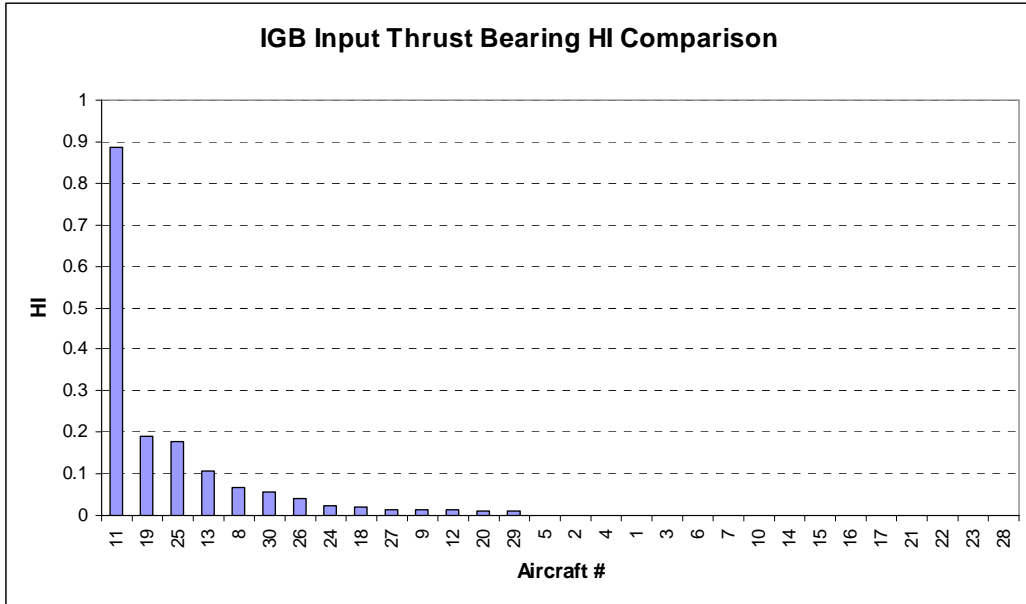


Figure 3. IGB Input Thrust Bearing HI comparison for the 30 aircraft. Aircraft # 11 has an elevated HI among 30 aircraft.

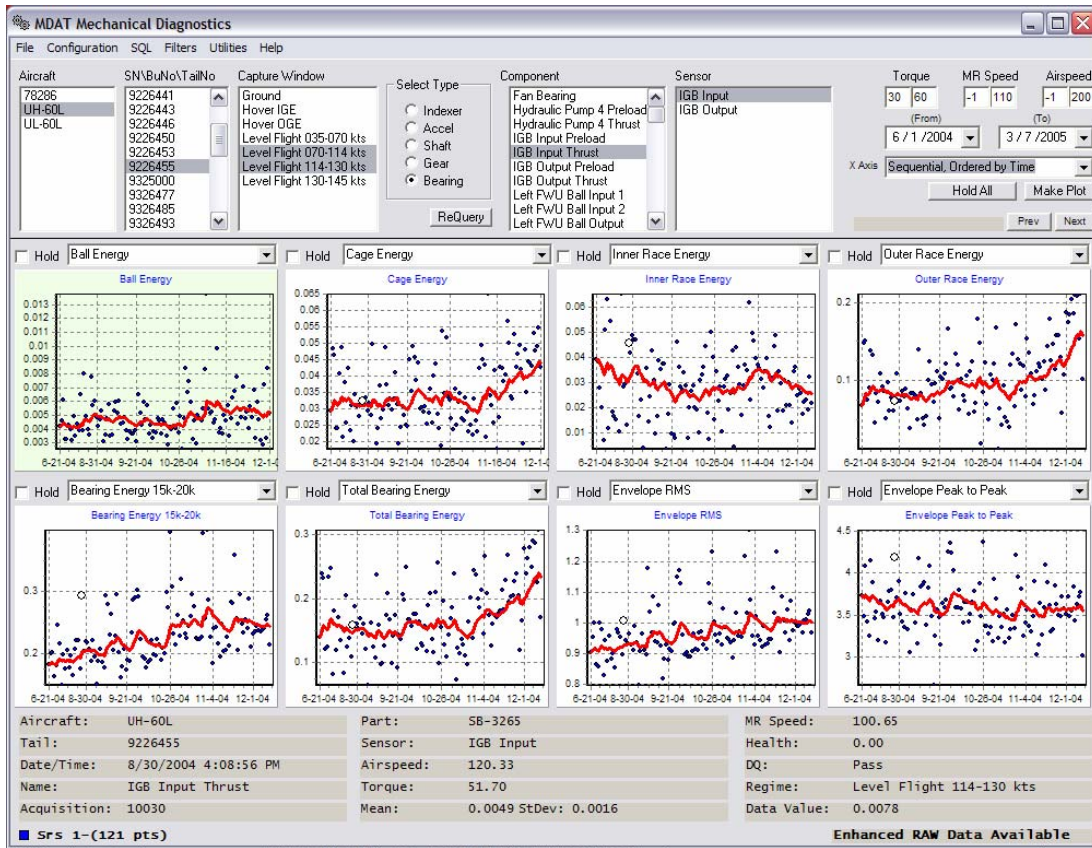


Figure 4. Goodrich MDAT Mechanical Diagnostics engineering tool showing CIs for the IGB Input Thrust Bearing for Aircraft # 11.

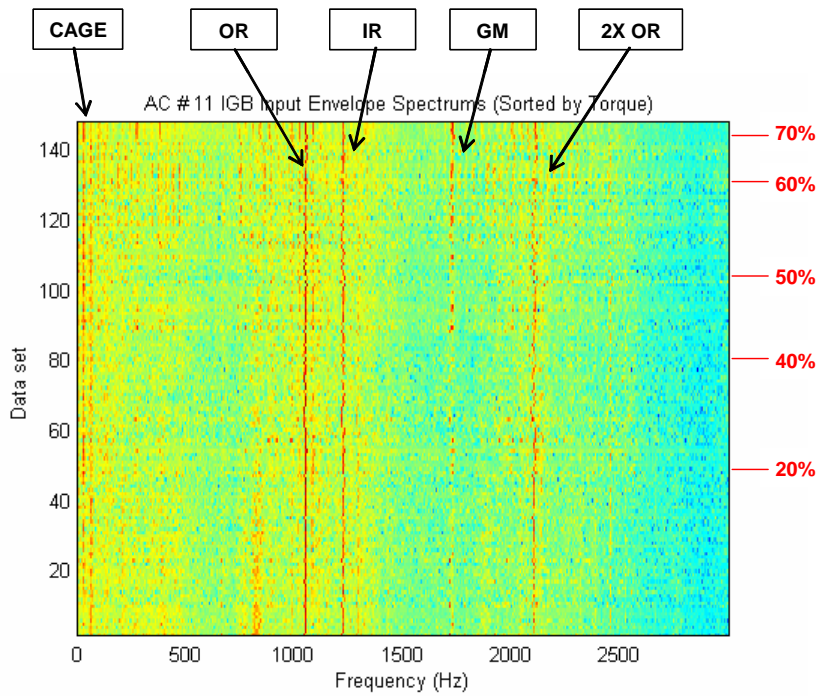


Figure 5. Topographical view of AC # 11 IGB Input Accelerometer envelope spectrums from 147 acquisitions.

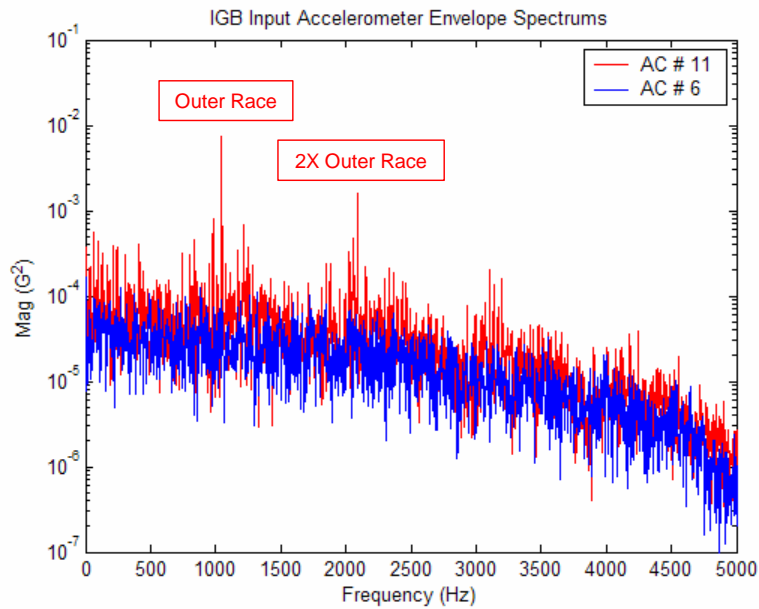


Figure 6. Envelope spectrum comparison between AC # 11 (with bearing defect tones) and AC # 6 (without bearing defect tones).

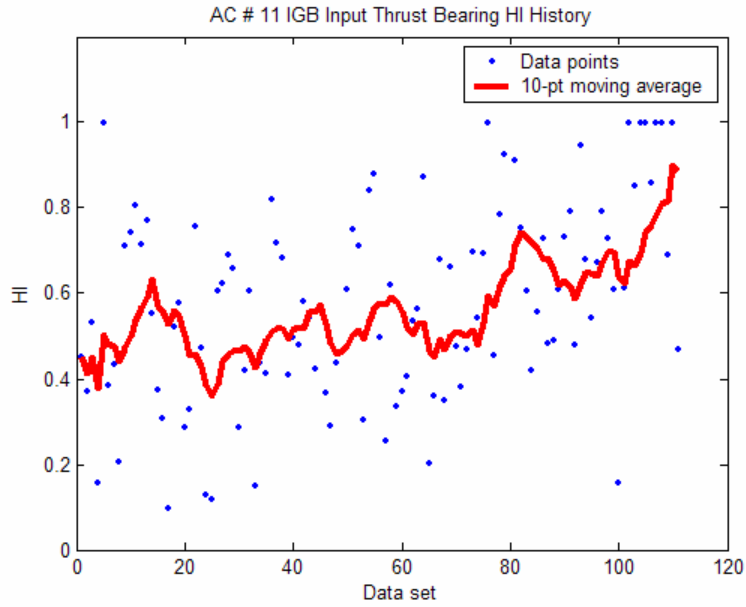


Figure 7. AC # 11 IGB Input Thrust Bearing HI time history showing an increasing trend.

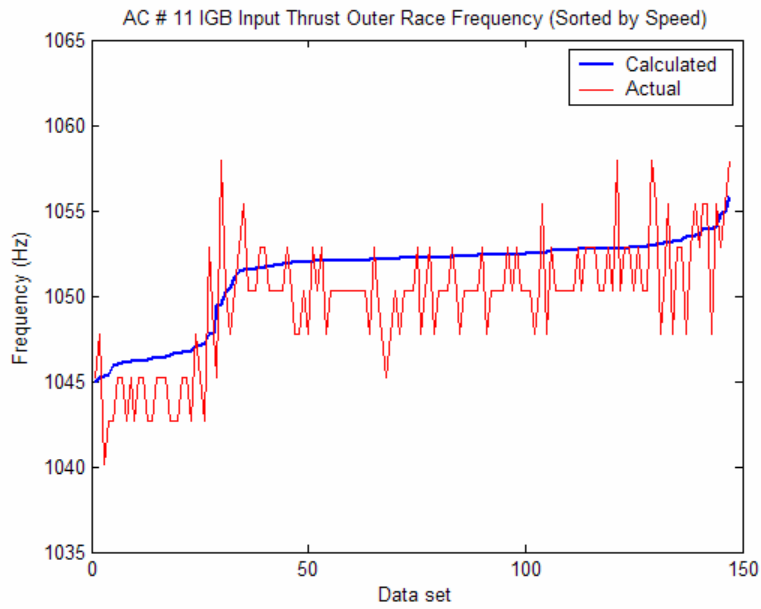


Figure 8. Comparison between calculated and actual IGB Input Thrust Bearing outer race frequencies at various shaft speeds. An offset between the actual and calculated frequencies is observed.

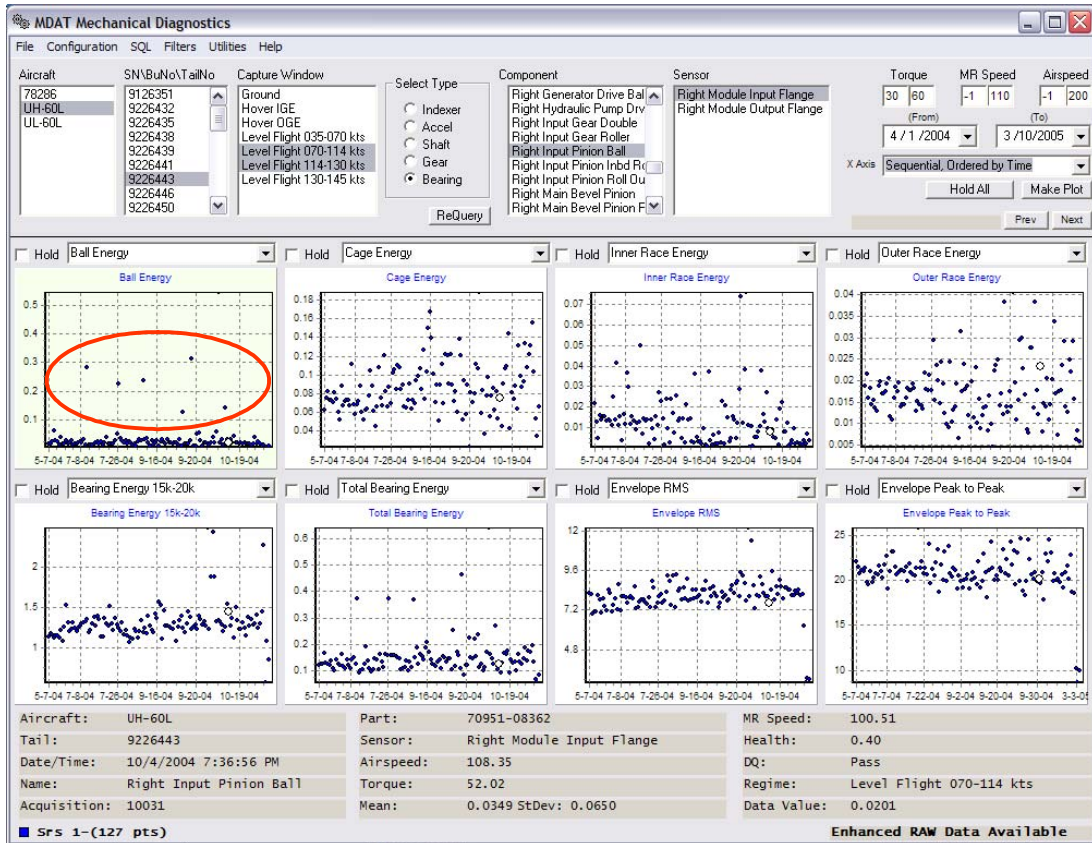


Figure 9. MDAT shows several elevated Ball Energy CI values (inside red ellipse) for AC #7 Right Module Input Spiral Bevel Pinion Gear Ball Bearing.

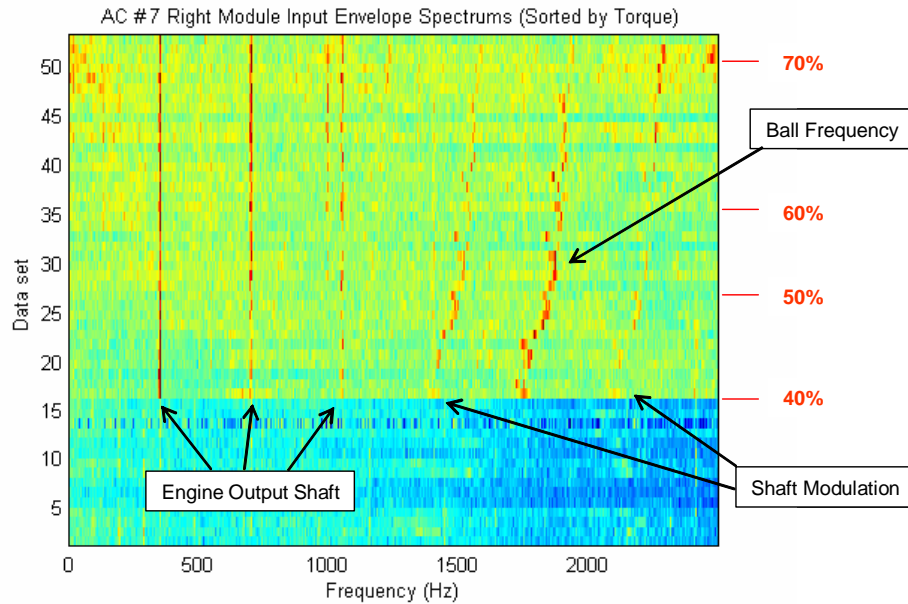


Figure 10. Topographical view of AC #7 Right Module Input Flange Accelerometer envelope spectrums from 53 acquisitions.

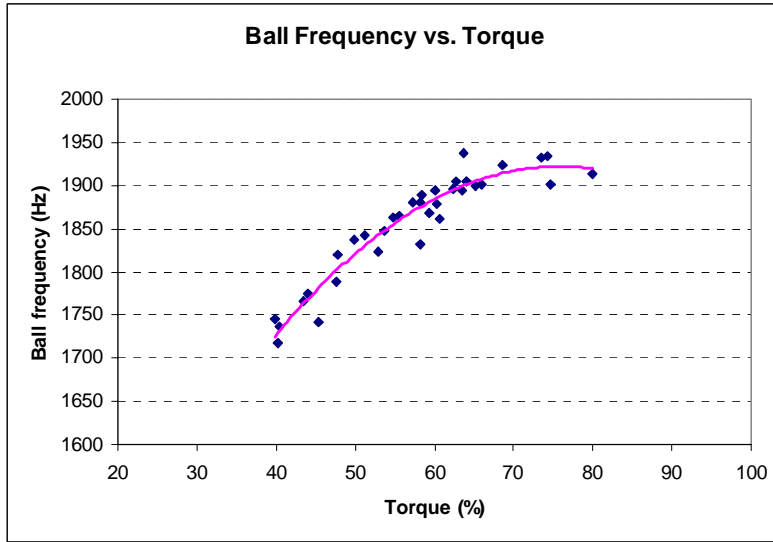


Figure 11. Ball frequency vs. engine torque for AC # 7 Right Module Input Spiral Bevel Pinion Gear Ball Bearing.